Sequence-dependent spin-selective tunneling along double-stranded DNA

Ai-Min Guo and Qing-feng Sun*
Institute of Physics, Chinese Academy of Sciences, Beijing 100190, China
(Received 1 August 2012; published 25 September 2012)

We report spin-selective tunneling of electrons along double-stranded DNA sandwiched between nonmagnetic leads. On the basis of a model Hamiltonian which contains spin-orbit interaction and dephasing, the conductance and the spin polarization are calculated for natural and artificial DNA molecules by using the Landauer-Büttiker formula. Our results reveal that the spin filtration efficiency strongly depends on the DNA sequence and is dominated by its end segment. Both genomic and artificial DNA molecules could be efficient spin filters. The spin-filtering effects are sensitive to point mutation which occurs in the end segment. These results are in good agreement with recent experiments and are robust against various types of disorder, and could help for designing DNA-based spintronic devices.

DOI: 10.1103/PhysRevB.86.115441 PACS number(s): 87.14.G−, 72.25.−b, 87.15.A−, 87.15.Pc

I. INTRODUCTION

Charge transport through DNA molecules has received significant attention from scientific researchers over the past two decades.[1–4] In addition to electric charges, the DNA molecule could be also used to manipulate electron spin. Recently, it was reported that self-assembled monolayers of double-stranded DNA (dsDNA) can discriminate the spin of photoelectrons,[5,6] which are ejected from the gold surface by ultraviolet (UV) light. These electrons transmitted through the dsDNA monolayers are highly polarized at room temperature and the spin-filtering effects are enhanced with increasing the DNA length.[6] Moreover, it was demonstrated that even single dsDNA could be an efficient spin filter by directly measuring its charge transport property.[7] This finding is surprising because the spin-orbit (SO) interaction is small in organic molecules that could not induce such high spin selectivity. The underlying physical mechanism can be attributed to the combination of the environment-induced dephasing, the SO coupling, and the chirality of the DNA molecule.[8] However, the spin polarization vanishes if the dsDNA is changed into single-stranded DNA or is damaged by the UV light.[6–8] Other theoretical models were also proposed to address the role of helical symmetry in the charge and spin transport properties.[9–12]

The nitrogenous bases guanine (G), adenine (A), cytosine (C), and thymine (T), which are four basic ingredients of the DNA molecule, can constitute thousands of various sequences. While natural DNA molecules can be extracted from the cells of all living organisms, artificial molecules could be synthesized in any desired sequence. It was shown that the DNA molecule with different sequences could present any transport behavior—conducting, semiconducting, and insulating.[13–16] One may thus expect that different dsDNA would display diverse spin-filtering effects. Indeed, the study of spin transport along various dsDNA will provide valuable information regarding the physical mechanism and the biological processes, and opens up potential applications in molecular spintronics. In this paper, we explore spin-selective tunneling of electrons through the dsDNA connected by normal-metal leads. Based on an effective model Hamiltonian which includes the SO coupling and the dephasing, conductance and spin polarization are calculated for a variety of dsDNA. In this work the DNA involves genomic and artificial molecules, as well as those employed in the experiments.[6,7] The sequences of several typical DNA samples are listed in Table I. The genomic dsDNA is extracted from the sequence of human chromosome 22 (chr22),[17] while the artificial dsDNA is taken as a random sequence and as substitutional, e.g., nickel mean (nm), copper mean (cm), triadic cantor (tc), and fibonacci (fb).[18] All of the substitutional DNA sequences are constructed by initiating from one seed and following a substitution rule. For instance, the nm1 sequence is formed by adopting base A as the seed and the substitution rule A → AGGG, G → A. Such sequences can be generated from the concatenation rule as well.[19]

From the study of numerous dsDNA molecules, we find that the spin filtration efficiency presents strong dependence on the DNA sequence and is mainly determined by the end segment with several base pairs. Both chr22-based and random dsDNA can be very efficient spin filters, while the substitutional dsDNA could exhibit large spin polarization and conductance. Besides, the spin-filtering effects are sensitive to point mutation which takes place in the end segment of the dsDNA. The high spin polarization still holds even under the environment-induced on-site energy disorder and twist angle disorder. These results could be beneficial for building up DNA-based spintronic devices.

The rest of the paper is organized as follows: In Sec. II, we present the theoretical model with parameters extracted from experimental results and first-principles calculations. In Sec. III, the spin polarization and the conductance are shown for various dsDNA sequences. Finally, the results are summarized in Sec. IV.

II. MODEL

The spin transport along the dsDNA can be described by the Hamiltonian:[8,20]

$$\mathcal{H} = \mathcal{H}_{\rm DNA} + \mathcal{H}_{\rm so} + \mathcal{H}_d + \mathcal{H}_{\rm lead} + \mathcal{H}_c. \quad (1)$$

Here, the first term $\mathcal{H}_{\rm DNA} = \sum_{j=1}^{2}(\sum_{n=1}^{N} \varepsilon_{jn} c_{jn}^{\dagger} c_{jn} + \sum_{n=1}^{N-1} t_{jn} c_{jn}^{\dagger} c_{jn+1}) + \sum_{n=1}^{N} \lambda_n c_{1n}^{\dagger} c_{2n} + \text{H.c.}$ is the Hamiltonian of the two-leg ladder model, with n the base-pair index, j the strand label, and N the DNA length. $c_{jn}^{\dagger} = (c_{jn\uparrow}^{\dagger}, c_{jn\downarrow}^{\dagger})$ is the creation operator, ε_{jn} is the on-site

TABLE I. The sequences of the DNA molecules. Here, only the sequence along one strand is presented, while the other can be derived according to Watson-Crick base-pairing rules: G pairs with C, and A with T. The first three terms are the DNA molecules adopted in the experiments, rd1, rd2, and rd3 are the random sequences, hc1, hc2, and hc3 are the chr22-based sequences, and the last six terms are the substitutional ones.

Name	DNA sequence
sq-26	TTTGTTTGTTTGTTTGTTTTTTTTTT
sq-40	TCTCAAGAATCGGCATTAGCTCAACTGTCAACTCCTCTTT
sq-50	TACTCTACCTTCTCAAGAATCGGCATTAGCTCAACTGTCAACTCCTCTTT
rd1	CAATGCAGTCTATCCACCTGACGGACCCCGACCCGCCTTT
rd2	CAATGCAGTCTATCCACCTGACGGACCCCGACCCGGCTTT
rd3	CAATGCAGTCTATCCACCTGACGGACCCCGACCCGCCATT
hc1	TAAATAAATAAATAAATAAATAAAATAAATAAAAGCCTTT
hc2	GGGCCCTGAGGCATGGGCCCAGAAGCATTCCTGTCCCCTT
hc3	AGCTGGGGAGCAGGGCTCCACTCTGGGAGGGGGGCAGCCT
nm1	AGGGAAAAGGGAGGGAGGGAGGGAAAAGGGAAAAGGGAAA
nm2	ATTTAAAATTTATTTATTTATTTAAAATTTAAAATTTAAA
cm	GAAGGGAAGAAGAAGGGAAGGGAAGGGAAGAAGAAGGGAA
tc	GAGAAAGAGAAAAAAAAAGAGAAAGAGAAAAAAAAAAAAA
fb1	AGAAGAGAAGAAGAGAAGAGAAGAAGAGAAGAAGAGAAGA
fb2	ATAATATAATAATATAATATAATAATATAATAATATAATA

energy, t_{jn} is the intrachain hopping integral, and λ_n is the interchain hybridization interaction.[21] The second term $\mathcal{H}_{\rm so} = \sum_{jn}\{it_{\rm so}c^{\dagger}_{jn}\sigma^{(j)}_{n}c_{jn+1} + \text{H.c.}\}$ is the SO Hamiltonian, which stems from the double-helix distribution of the electrostatic potential of the dsDNA.[8] $t_{\rm so}$ is the SO coupling strength and $\sigma^{(j)}_{n} = [\sigma_x(\sin\varphi_{jn} + \sin\varphi_{jn+1}) - \sigma_y(\cos\varphi_{jn} + \cos\varphi_{jn+1})]\sin\theta_{jn} + 2\sigma_z\cos\theta_{jn}$, with $\sigma_{x,y,z}$ the Pauli matrices, φ_{jn} the cylindrical coordinate of the base, and θ_{jn} the helix angle between base n and $n+1$ in the jth strand.[8] In the equilibrium position of the dsDNA, $\varphi_{jn} = (n-1)\Delta\varphi$ and $\theta_{jn} = \theta$ with $\Delta\varphi$ the twist angle. The third one, $\mathcal{H}_d = \sum_{jnk}(\varepsilon_{jnk}b^{\dagger}_{jnk}b_{jnk} + t_d b^{\dagger}_{jnk}c_{jn} + \text{H.c.})$, is the Hamiltonian of the Büttiker's virtual leads and their coupling with each base of the dsDNA, simulating the phase-breaking processes due to the inelastic scattering with phonons and counterions.[22,23] The last two terms $\mathcal{H}_{\rm lead} + \mathcal{H}_c = \sum_{k,\beta=L,R}\varepsilon_{\beta k}a^{\dagger}_{\beta k}a_{\beta k} + \sum_{jk}(t_L a^{\dagger}_{Lk}c_{j1} + t_R a^{\dagger}_{Rk}c_{jN} + \text{H.c.})$ represent the real leads and the coupling between these leads and the dsDNA, respectively.

The conductances for spin-up ($G_\uparrow$) and spin-down ($G_\downarrow$) electrons can be calculated by using the Landauer-Büttiker formula.[8] The spin polarization is $P_s = (G_\uparrow - G_\downarrow)/(G_\uparrow + G_\downarrow)$. Since the current is flowing from the left real lead to the right one, the terminal of the dsDNA attached to the former is named the beginning, while the other terminal is called the end.

For the dsDNA, ε_{jn} is chosen as the ionization potential with $\varepsilon_{\rm G} = 8.3$, $\varepsilon_{\rm A} = 8.5$, $\varepsilon_{\rm C} = 8.9$, and $\varepsilon_{\rm T} = 9.0$; t_{jn} between identical neighboring bases is taken as $t_{\rm GG} = 0.11$, $t_{\rm AA} = 0.22$, $t_{\rm CC} = -0.05$, and $t_{\rm TT} = -0.14$; and $\lambda_n = -0.3$. These parameters are extracted from the experimental results[24–27] and first-principles calculations[28–34] with units in electronvolts. t_{jn} between different neighboring bases X and Y is set to $t_{XY} = (t_{XX} + t_{YY})/2$, in accordance with first-principles results.[30–33] The helix angle and the twist one are $\theta = 0.66$ rad and $\Delta\varphi = \frac{\pi}{5}$. The SO coupling is estimated to $t_{\rm so} = 0.01$. For the real leads, the parameters $\Gamma_L = \Gamma_R = 1$ are fixed, while for the virtual ones, the dephasing strength is $\Gamma_d = 0.006$. The values of all these parameters will be used throughout this paper, except for Fig. 2(d), of which the inset is performed with $\Gamma_d = 0.01$. In fact, our results still hold by changing the model parameters in a wide range.

III. RESULTS AND DISCUSSION

It was reported that the ionization potential of the base is affected significantly by both counterions[35,36] and hydration.[37–39] Consequently, the environmental effects can be properly considered by varying the on-site energies. A random variable w_{jn} is added in each ε_{jn} to simulate the stochastic population of these counterions and water molecules around the dsDNA, with w_{jn} uniformly distributed within the range $[-\frac{W}{2}, \frac{W}{2}]$ and W the disorder degree. Figure 1(a) shows the spin polarization P_s of poly(A)-poly(T) under the on-site energy disorder, as a function of the energy E. It clearly appears that P_s is large for homogeneous poly(A)-poly(T) and is sufficiently robust against the on-site energy disorder. This can be further demonstrated in Fig. 1(c), where the averaged spin polarization $\langle P_s\rangle$ is shown. One notices that $\langle P_s\rangle$ fluctuates around its equilibrium value of 5.0% at $W = 0$ and the oscillation amplitude is enhanced by W. Furthermore, a new energy region of high P_s becomes more distinct in the case of larger W [see the curves of $W = 0.16$ and 0.3 in Fig. 1(a)]. On the other hand, the averaged conductance $\langle G_\uparrow\rangle$ is decreased by increasing W as expected, due to the disorder-induced Anderson localization effect. The curve of $\langle G_\uparrow\rangle$-$W$ can be fitted well by a simple function $\langle G_\uparrow\rangle \propto 10^{-\alpha W}$ [see inset of Fig. 1(c)].

Besides the on-site energy disorder, each base will waver around its equilibrium position at finite temperature. In this situation, it is reasonable to plus a random variable d_{jn} in each φ_{jn}, with d_{jn} distributed in the region $[-\frac{D}{2}, \frac{D}{2}]$ and D

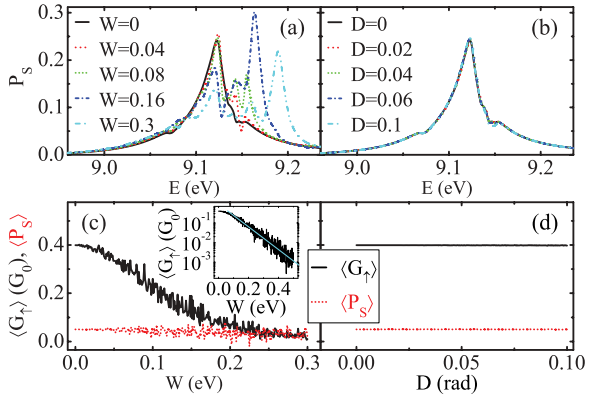

FIG. 1. (Color online) Energy-dependent P_s for poly(A)-poly(T) under the on-site energy disorder with degree W (a) and of the twist angle disorder with degree D (b). $\langle G_\uparrow \rangle$ and $\langle P_s \rangle$ vs W (c) and vs D (d). The inset of (c) shows $\langle G_\uparrow \rangle$ in a wider range of W, and the dependence can be fitted by the function $\langle G_\uparrow \rangle \propto 10^{-\alpha W}$ with $\alpha = 5.80 \pm 0.09$ (cyan line). $\langle G_\uparrow \rangle$ and $\langle P_s \rangle$ are averaged in the energy region [9.04,9.32]. All of the results are performed for single-disorder configuration with $N = 40$ and are similar for other disorder configurations. Here, $G_0 = e^2/h$ is the quantum conductance.

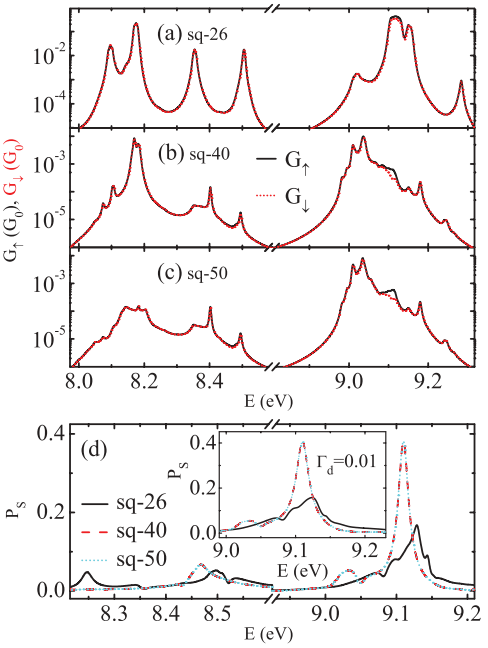

FIG. 2. (Color online) Energy dependence of $G_\uparrow$, $G_\downarrow$, and P_s for the dsDNA used in the experiments. $G_\uparrow$ and $G_\downarrow$ for the sq-26 sequence (a), the sq-40 one (b), and the sq-50 one (c). (d) P_s for all three dsDNA. The inset of (d) displays P_s with $\Gamma_d = 0.01$.

the disorder degree. By considering constant radius R of the dsDNA and arc length l_a between successive bases to account for the rigid sugar-phosphate backbone,[8,40] the helix angle θ_{jn} will be modulated according to $l_a \cos\theta_{jn} = R(\varphi_{jn+1} - \varphi_{jn})$ and the fluctuations are disregarded in the intrachain hopping integral as a first approximation.[32,41,42] It can be seen from Fig. 1(b) that the curves of P_s-E are almost superposed with each other in the context of the twist angle disorder only. Accordingly, no fluctuations could be observed in the curve of $\langle P_s \rangle$-D [Fig. 1(d)]. Besides, $\langle G_\uparrow \rangle$ will not be changed with D, because the SO coupling is much smaller than the hopping integral. Therefore, poly(A)-poly(T) remains an efficient spin filter, even under the on-site energy disorder and the twist angle disorder.

Then we investigate the spin transport through aperiodic dsDNA in the absence of external environment-induced disorder. Our results still hold if the on-site energy disorder or the twist angle disorder is included. Let us first discuss the spin transport properties of the dsDNA used in the experiments.[6,7] Figures 2(a)–2(c) display the conductances of spin-up ($G_\uparrow$) and spin-down ($G_\downarrow$) electrons for sq-26, sq-40, and sq-50 sequences, respectively. As compared with homogeneous dsDNA,[8] the energy spectrum of aperiodic dsDNA is also separated into the highest occupied molecular orbital (HOMO) and the lowest unoccupied molecular orbital (LUMO). The conductance is declined by increasing the DNA length, because the electrons experience stronger scattering in longer dsDNA.

In addition, one can see from Figs. 2(a)–2(c) that the discrepancy between $G_\uparrow$ and $G_\downarrow$ is more distinct for the LUMO band than the HOMO one. Thus, P_s is larger in the former band than the latter one [Fig. 2(d)]. Moreover, P_s at $E = 9.11$ is, respectively, 9.6%, 38%, and 38% for the sq-26, sq-40, and sq-50 sequences, in good agreement with the experiment.[6] In fact, the obtained P_s is also consistent with the experimental results by adopting different Γ_d from the region [0.003,0.01], e.g., see P_s of $\Gamma_d = 0.01$ in the inset of Fig. 2(d). Besides, although the conductances between the sq-40 and sq-50 sequences are very different, their spin polarizations are almost identical and the difference between the two P_s is within 10^{-6} range, due to the fact that the sq-40 sequence is the end part of the sq-50 sequence. This suggests that the spin filtration efficiency of the dsDNA is mainly controlled by its end segment, which will be substantiated below.

Next we study the spin polarization of the random and chr22-based dsDNA. Figures 3(a) and 3(b) plot P_s vs E for several typical random and chr22-based sequences, respectively. It is clear from the curves of rd1 and hc1 that both random and chr22-based sequences could be very efficient spin filters with P_s achieving 40%. From a statistical study of numerous dsDNA with extremely high P_s, it reveals that these sequences are usually terminated by the segment "CCTTT/GGAAA" in their ends [Fig. 3(c)]. We emphasize that all of the investigated dsDNA with $N = 40$ will exhibit very high P_s values of around 40% if their end segments are replaced by "CCTTT/GGAAA". Besides, the dsDNA could also be a very efficient spin filter if it has other end segments, as shown in Fig. 3(c), where a distribution of P_s at $E = 9.11$ is displayed for different random dsDNA with 16 end segments. It clearly appears that P_s is always large for these dsDNA [see the right part in Fig. 3(c)], although P_s will vary in a finite range. The dsDNA remains an efficient spin filter if it is ended by the moiety "$(C)_m TT/(G)_m AA$", with m the integer (see the curve of hc2). However, P_s can be dramatically reduced by altering the end segment, even if its last base pair is changed [see the left part in Fig. 3(c)]. These are due to the fact that the charge will gradually lose its phase and spin memory while

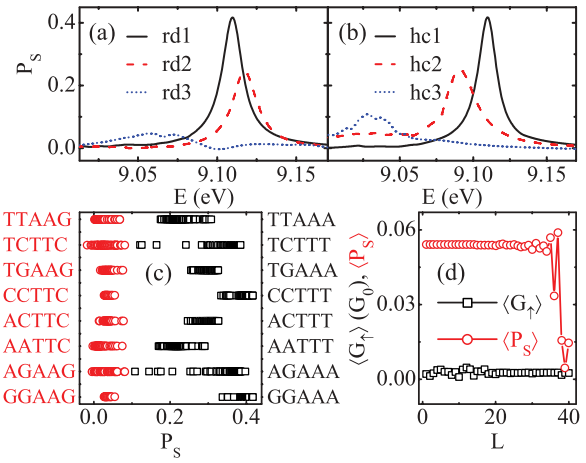

FIG. 3. (Color online) Energy-dependent P_s for the random dsDNA (a) and for the chr22-based one (b). (c) Distribution of P_s at $E = 9.11$ for various random dsDNA with large P_s (right part) and with small P_s (left part) as a comparison. The results are extracted from 10^5 DNA samples. Here, only the end segment in the first strand is shown (two sides) and can be obtained for the second one according to the base-pairing rules. For instance, the moiety "CCTTT" denotes "CCTTT/GGAAA" in the dsDNA. (d) $\langle G_\uparrow \rangle$ and $\langle P_s \rangle$ vs mutation position L for the rd1 sequence.

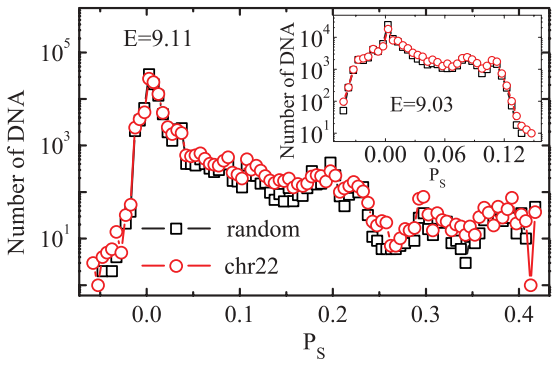

FIG. 4. (Color online) Distribution functions of P_s for the random and chr22-based dsDNA at $E = 9.11$. The inset shows the corresponding statistics of P_s at $E = 9.03$. Here, $N = 40$.

transmitting along the dsDNA. The longer distance the charge propagates, the larger the loss of its memory. Accordingly, the spin filtration efficiency of the dsDNA is dominated by its end segment containing several base pairs.

To further verify the aforementioned point, we introduce point mutation in the dsDNA, where only one base pair is modified and replaced by another.[43,44] Here, the point mutation is defined by switching the complementary bases within a single base pair.[45] We focus on P_s of the random dsDNA in Fig. 3(a). The rd2 and rd3 sequences are derived by introducing the point mutation in the rd1 sequence.[45] One notes that P_s is reduced more significantly if the mutation position is closer to the last base pair of the rd1 sequence. The largest P_s is decreased from 42% for the rd1 sequence to 25% and 4.7% for the rd2 and rd3 sequences, respectively. $\langle P_s \rangle$ and $\langle G_\uparrow \rangle$ are shown as a function of the mutation position L in Fig. 3(d), where the average is obtained within the energy region [8.98,9.18]. It is clear that $\langle P_s \rangle$ does not change if the mutation occurs in the very beginning of the rd1 sequence, and fluctuates more strongly if the mutation position becomes closer to its end. P_s is very small if the point mutation takes place within the last three base pairs, due to the identical sign between t_{1n} and t_{2n}.[8] In contrast, $\langle G_\uparrow \rangle$ fluctuates more obviously if the mutation occurs in the beginning of the sequence, and the fluctuation amplitude is more severe in the curve of $\langle P_s \rangle$-L than $\langle G_\uparrow \rangle$-$L$, indicating that the spin polarization is much more sensitive to the modification of the base pair in the dsDNA than the conductance. In this perspective, the spin transport along the dsDNA may be related to mutation detection in the biological processes and could be beneficial for DNA sequencing.[46]

Figure 4 shows the statistical properties of P_s at fixed energy for the random and chr22-based dsDNA with 10^5 samples. It clearly appears that P_s can vary from 42% to negative, implying that the spin-polarization direction of the charges transmitted through the dsDNA could be reversed by modifying its sequence, and one can see that many DNA molecules exhibit high P_s. From a statistical perspective, the chr22-based dsDNA has more efficient spin filters than the random one. For instance, the number of the dsDNA, of which P_s is larger than 30% (20%), is 458 (1436) and 667 (2020) for the random dsDNA and the chr22-based one, respectively. This can be further demonstrated in the inset of Fig. 4, where one notices that the curve of the chr22-based dsDNA is always higher than that of the random one for $P_s > 1.3\%$. However, there are also many dsDNA with small P_s at fixed energy. This is attributed to the fact that (1) P_s depends on E that the energy region of large P_s may differ from one sample to another [Figs. 3(a) and 3 (b)], and (2) the electrons may not be polarized exactly along the helix axis for each dsDNA and the actual spin polarization could be larger.

Finally, we study the spin polarization of the substitutional DNA molecules, of which the electronic properties have been investigated previously.[19,47] Figure 5 shows P_s and $G_\uparrow$ for several substitutional dsDNA. It is clear that besides homogeneous DNA molecules, some substitutional dsDNA can also be efficient spin filters with high spin polarization and conductance. One can see that $G_\uparrow$ are very large for

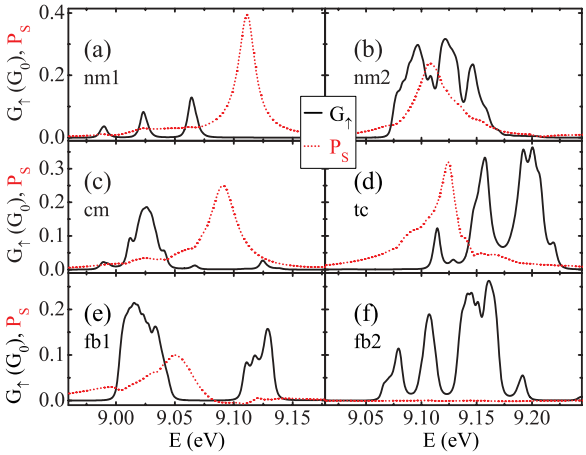

FIG. 5. (Color online) Energy dependence of $G_\uparrow$ and P_s for several substitutional sequences of DNA molecules.

all these dsDNA, due to the long-range correlations.[19,47] The nm1 sequence has the largest P_s as that of the rd1 and hc1 sequences, while P_s of the cm sequence is almost identical to that of the hc2 one [see Figs. 3(a) and 3(b)]. Additionally, the spin-polarization configurations of the tc sequence and poly(A)-poly(T) are similar to each other. P_s at $E = 9.11$ of the nm2 sequence is within its range for the dsDNA of the end segment "TTAAA/AATTT" [see Fig. 3(c)]. All of these further demonstrate that the spin filtration efficiency of the dsDNA is determined by its end segment and does not have obvious relation with its sequence correlations. Besides, P_s will differ from one substitutional dsDNA to another and can be small for the correlated dsDNA [Figs. 5(e) and 5(f)].

IV. CONCLUSIONS

In summary, we investigate the quantum spin transport through different dsDNA contacted by nonmagnetic leads. We find that the spin polarization strongly depends on the dsDNA sequence and is mainly determined by the end segment. Both natural and artificial dsDNA could be very efficient spin filters. Our results could motivate further experimental studies on DNA spintronics.

ACKNOWLEDGMENTS

This work was financially supported by NBRP of China (2012CB921303 and 2009CB929100) and NSF-China under Grants No. 10974236 and No. 11074174.

*sunqf@iphy.ac.cn

[1] C. Dekker and M. A. Ratner, Phys. World **14**, 29 (2001).
[2] R. G. Endres, D. L. Cox, and R. R. P. Singh, Rev. Mod. Phys. **76**, 195 (2004).
[3] J. C. Genereux and J. K. Barton, Chem. Rev. **110**, 1642 (2010).
[4] R. Naaman and D. H. Waldeck, J. Phys. Chem. Lett. **3**, 2178 (2012).
[5] S. G. Ray, S. S. Daube, G. Leitus, Z. Vager, and R. Naaman, Phys. Rev. Lett. **96**, 036101 (2006).
[6] B. Göhler, V. Hamelbeck, T. Z. Markus, M. Kettner, G. F. Hanne, Z. Vager, R. Naaman, and H. Zacharias, Science **331**, 894 (2011).
[7] Z. Xie, T. Z. Markus, S. R. Cohen, Z. Vager, R. Gutierrez, and R. Naaman, Nano Lett. **11**, 4652 (2011).
[8] A.-M. Guo and Q.-F. Sun, Phys. Rev. Lett. **108**, 218102 (2012).
[9] S. S. Skourtis, D. N. Beratan, R. Naaman, A. Nitzan, and D. H. Waldeck, Phys. Rev. Lett. **101**, 238103 (2008).
[10] S. Yeganeh, M. A. Ratner, E. Medina, and V. Mujica, J. Chem. Phys. **131**, 014707 (2009).
[11] R. Gutierrez, E. Díaz, R. Naaman, and G. Cuniberti, Phys. Rev. B **85**, 081404(R) (2012).
[12] D. Vager and Z. Vager, Phys. Lett. A **376**, 1895 (2012).
[13] Y. Zhang, R. H. Austin, J. Kraeft, E. C. Cox, and N. P. Ong, Phys. Rev. Lett. **89**, 198102 (2002).
[14] E. Shapir, H. Cohen, A. Calzolari, C. Cavazzoni, D. A. Ryndyk, G. Cuniberti, A. Kotlyar, R. Di Felice, and D. Porath, Nat. Mater. **7**, 68 (2008).
[15] X. Guo, A. A. Gorodetsky, J. Hone, J. K. Barton, and C. Nuckolls, Nat. Nanotechnol. **3**, 163 (2008).
[16] J. D. Slinker, N. B. Muren, S. E. Renfrew, and J. K. Barton, Nat. Chem. **3**, 228 (2011).
[17] We consider the largest segment in the human chromosome 22 sequence, which is retrieved from the National Center for Biotechnology Information (accession number NT011520).
[18] E. Maciá, Rep. Prog. Phys. **69**, 397 (2006).
[19] A.-M. Guo, Phys. Rev. E **75**, 061915 (2007).
[20] A.-M. Guo and Q.-F. Sun, Phys. Rev. B **86**, 035424 (2012).
[21] Here, the electron-electron interaction is neglected. When it is considered, the Coulomb blockade may occur and improve the spin polarization, because the majority spin electrons can be injected into the dsDNA more easily and then block the minority spin electrons. This case is similar to the spin polarization in a quantum dot, see Q.-F. Sun and X. C. Xie, Phys. Rev. B **73**, 235301 (2006).
[22] Y. A. Berlin, A. L. Burin, and M. A. Ratner, J. Am. Chem. Soc. **123**, 260 (2001).
[23] Y. A. Berlin, A. L. Burin, and M. A. Ratner, Chem. Phys. **275**, 61 (2002).
[24] N. S. Hush and A. S. Cheung, Chem. Phys. Lett. **34**, 11 (1975).
[25] D. Dougherty, K. Wittel, J. Meeks, and S. P. McGlynn, J. Am. Chem. Soc. **98**, 3815 (1976).
[26] J. Lin, C. Yu, S. Peng, I. Akiyama, K. Li, L. K. Lee, and P. R. LeBreton, J. Phys. Chem. **84**, 1006 (1980).
[27] A. B. Trofimov, J. Schirmer, V. B. Kobychev, A. W. Potts, D. M. P. Holland, and L. Karlsson, J. Phys. B **39**, 305 (2006).
[28] E. M. Conwell and S. V. Rakhmanova, Proc. Natl. Acad. Sci. USA **97**, 4556 (2000).
[29] F. C. Grozema, Y. A. Berlin, and L. D. A. Siebbeles, J. Am. Chem. Soc. **122**, 10903 (2000).
[30] A. A. Voityuk, J. Jortner, M. Bixon, and N. Rösch, J. Chem. Phys. **114**, 5614 (2001).
[31] H. Zhang, X.-Q. Li, P. Han, X. Y. Yu, and Y. Yan, J. Chem. Phys. **117**, 4578 (2002).
[32] K. Senthilkumar, F. C. Grozema, C. F. Guerra, F. M. Bickelhaupt, F. D. Lewis, Y. A. Berlin, M. A. Ratner, and L. D. A. Siebbeles, J. Am. Chem. Soc. **127**, 14894 (2005).
[33] L. G. D. Hawke, G. Kalosakas, and C. Simserides, Eur. Phys. J. E **32**, 291 (2010).
[34] V. Apalkov, J. Berashevich, and T. Chakraborty, J. Chem. Phys. **132**, 085102 (2010).
[35] R. N. Barnett, C. L. Cleveland, A. Joy, U. Landman, and G. B. Schuster, Science **294**, 567 (2001).
[36] Y. Zhu, C.-C. Kaun, and H. Guo, Phys. Rev. B **69**, 245112 (2004).
[37] S. K. Kim, W. Lee, and D. R. Herschbach, J. Phys. Chem. **100**, 7933 (1996).
[38] X. Yang, X.-B. Wang, E. R. Vorpagel, and L.-S. Wang, Proc. Natl. Acad. Sci. USA **101**, 17588 (2004).
[39] L. Belau, K. R. Wilson, S. R. Leone, and M. Ahmed, J. Phys. Chem. A **111**, 7562 (2007).
[40] J. Gore, Z. Bryant, M. Nöllmann, M. U. Le, N. R. Cozzarelli, and C. Bustamante, Nature (London) **442**, 836 (2006).
[41] S. Roche, Phys. Rev. Lett. **91**, 108101 (2003).

[42]R. Gutiérrez, R. A. Caetano, B. P. Woiczikowski, T. Kubar, M. Elstner, and G. Cuniberti, Phys. Rev. Lett. **102**, 208102 (2009).
[43]C.-T. Shih, S. Roche, and R. A. Römer, Phys. Rev. Lett. **100**, 018105 (2008).
[44]C.-T. Shih, S. A. Wells, C.-L. Hsu, Y.-Y. Cheng, and R. A. Römer, Sci. Rep. **2**, 272 (2012).
[45]The rd2 and rd3 sequences are transformed from the rd1 sequence. We obtain the former two sequences by substituting the 36th base pair C/G with G/C and the 38th base pair T/A with A/T, respectively.
[46]M. Zwolak and M. Di Ventra, Rev. Mod. Phys. **80**, 141 (2008).
[47]S. Roche, D. Bicout, E. Maciá, and E. Kats, Phys. Rev. Lett. **91**, 228101 (2003).